



Significant improvement of soft magnetic properties for Fe(Co)BPSiC amorphous alloys by magnetic field annealing



Chengliang Zhao ^{a, b, c}, Anding Wang ^{a, d, *}, Shiqiang Yue ^{a, b}, Tao Liu ^{a, b, c}, Aina He ^{a, b, **}, Chuntao Chang ^{a, b}, Xinmin Wang ^{a, b, ***}, Chain-Tsuan Liu ^d

^a Key Laboratory of Magnetic Materials and Devices, Ningbo Institute of Materials Technology and Engineering, Chinese Academy of Sciences, Ningbo, Zhejiang, 315201, China

^b Zhejiang Province Key Laboratory of Magnetic Materials and Application Technology, Ningbo Institute of Materials Technology and Engineering, Chinese Academy of Sciences, Ningbo, 315201, China

^c University of Chinese Academy of Sciences, 19 A Yuquan Rd, Shijingshan District, Beijing, 100049, China

^d Center for Advanced Structural Materials, Department of Mechanical and Biomedical Engineering, College of Science and Engineering, City University of Hong Kong, Kowloon, Hong Kong, China

ARTICLE INFO

Article history:

Received 30 July 2017

Received in revised form

11 January 2018

Accepted 23 January 2018

Available online 31 January 2018

Keywords:

Amorphous alloy

Field annealing

Curie temperature

Soft magnetic property

Magnetic domain

ABSTRACT

Longitudinal field annealing (FA) is used to improve the soft magnetic properties (SMPs) of Fe_{83-x}Co_xB₁₁P₃Si₂C₁ ($x = 0-20$) amorphous alloys with high B_s of 1.65–1.76 T. These amorphous ribbons after FA exhibit pronouncedly improved SMPs, including low coercivity of 1.0–2.3 A/m and high permeability of 6.6–13 × 10³ at 1 kHz. In comparison with normal annealing (NA), FA is found to be an effective process in improving the SMPs for all amorphous alloys. While NA is only effective for the alloys with T_c lower than the onset temperature of the crystallization (T_{X1}). It is also found that FA can change the domain sensitive direction from transversal to along the ribbon axis, and unify the easy magnetization direction. This mechanistically explains the positive effects of applied field on SMPs and structure relaxation. This paper will give a better understanding of relaxation effect on SMPs and a prospective view in formulating heat-treatment process of the thin ribbons fabricated by using a single roller melt spinning process.

© 2018 Elsevier B.V. All rights reserved.

1. Introduction

Fe-based amorphous alloy ribbons fabricated by using a single roller melt spinning process have been widely used in electrical and electronic devices including transformers, motors etc., owing to their high saturated magnetic flux density (B_s), low coercivity (H_c), high permeability (μ_e) and low core loss [1,2]. Compared with traditional Si-steel, amorphous alloys possess relatively lower B_s

(~lower than 1.65 T), which hampers the miniature of the devices [3,4]. Developing higher B_s amorphous alloys with low H_c , becomes a most important issue for scientific and technological researches [5].

There are three main ways to increase B_s of Fe-based amorphous alloys, including increasing Fe content [6], substitution of Fe with Co [7] and nanocrystallization by annealing [8]. The Fe content is limited because of its balance to the AFA. The nanocrystallization of high B_s amorphous alloys has been found to suffer the non-uniform microstructure and poor manufacturability. The partial substitution of Fe with Co is an effective method to increase B_s without decreasing GFA or decreasing the manufacturability. It has been used to develop high B_s amorphous alloys [9,10]. As documented, the Co-doping in some cases can enhance the SMPs, glass forming ability and B_s [11,12]. While in other cases, Co addition leads to deteriorated SMPs after normal annealing (NA), especially for high FeCo content alloys [9,10,13]. For the later situation, Co was found to increase the anisotropy and T_c , resulting in deteriorated SMPs especially when NA at temperature lower than T_c [10]. Further

* Corresponding author. Key Laboratory of Magnetic Materials and Devices, Ningbo Institute of Materials Technology and Engineering, Chinese Academy of Sciences, Ningbo, Zhejiang, 315201, China.

** Corresponding author. Key Laboratory of Magnetic Materials and Devices, Ningbo Institute of Materials Technology and Engineering, Chinese Academy of Sciences, Ningbo, Zhejiang, 315201, China.

*** Corresponding author. Key Laboratory of Magnetic Materials and Devices, Ningbo Institute of Materials Technology and Engineering, Chinese Academy of Sciences, Ningbo, Zhejiang, 315201, China.

E-mail addresses: anding@nimte.ac.cn (A. Wang), hean@nimte.ac.cn (A. He), jbmwang@yahoo.co.jp (X. Wang).

understanding the effect of Co addition and exploring effective process for improving SMPs of the high B_s alloys enhanced by Co-addition are hence indispensable. Essentially, the excellent SMPs of ferromagnetic amorphous alloys are originated from the homogenous structure and eliminated inner stress without crystallization or clustering after annealing. The influence of Co addition on SMPs should naturally conduct during the annealing induced relaxation process and correlate to the inner magnetic field effect [14,15]. Consideration of the scientifically interesting issue of structure relaxation with introduction of inner magnetic field may help us to deep understand this critical question and find solutions [14,15]. In addition, FA is reported to be effective in ordering the magnetic moment and tailoring the domain structure [15,16], which can be applied to affect the anisotropy. Neutralizing the negative effect of inner magnetic field by applied magnetic field may be a feasible technique, which mechanism is quite urgent to be unveiled.

In this study, $\text{Fe}_{83-x}\text{Co}_x\text{B}_{11}\text{P}_3\text{Si}_2\text{C}_1$ ($x=0-20$) amorphous alloy ribbons fabricated by using a single roller melt spinning process with high B_s and significantly different $T_{x1} - T_c$ were selected and subjected to NA and FA. The Co content effect on thermal parameters and NA/FA effects on SMPs were systematically studied. The magnetic domain structures after NA and FA were further investigated to explore the mechanism of NA and FA effects on the SMPs. Here we propose a physical picture of the structure transition during relaxation for the alloys affected by inner and applied magnetic fields. This work will bring a new perspective to understand the effect of annealing induced structure relaxation and a guidance for the SMPs adjustment of ferromagnetic BMGs.

2. Experimental procedure

Alloys with compositions of $\text{Fe}_{83-x}\text{Co}_x\text{B}_{11}\text{P}_3\text{Si}_2\text{C}_1$ alloys ($x=0, 5, 10, 15$ and 20) were prepared with induction melting by mixing pure elements of Fe (99.99%), Co (99.9%), Si (99.99%), B (99.9%) and pre-alloyed Fe_3P and $\text{Fe}-3.6\%\text{C}$ ingots under an argon atmosphere. Ribbons with width of about 1 mm and thickness of about $25\ \mu\text{m}$ were prepared with commonly used single roller spinning method and parameters. Thermal parameters including crystallization temperature (T_x) and Curie temperature (T_c) were analyzed by thermal gravity and differential thermal analysis (TG/DTA, PerkinElmer Diamond) at a heating rate of 10 K/min under protection of N_2 . Ribbon samples with length of about 50 mm were cut for isothermal FA and NA annealing under 633 K for 15 min. As schematically shown in Fig. 2(a), FA and NA was conducted in a quartz ampoule with an inner diameter of 25 mm and a thickness of about 1.5 mm filled with argon. The isothermal treatment process includes: 1) fix the ribbon sample in a holder made with quartz glass with a thickness of 1 mm and then seal in the quartz ampoule, 2) push the electric tube furnace with a preset temperature, 3) pull out the tube and 4) quench them in water to room temperature. The heating and cooling rates were not constant values. At each side of the sample holder, an AlNiCo magnet with high operating temperature of over 800 K was used to provide a magnetic field of about 200 Oe along the FA ribbons. For NA annealing, the thermally demagnetic AlNiCo magnets were used for comparison. The domain structures were characterized via the Magneto-optical Kerr Microscope (MOKE, Evico 4-873K/950 MT) without taking SMP tests. Ribbons (50 mm in length) for SMPs (H_c and μ_e) were measured by using a DC B-H loop tracer (Riken Denshi DC BHS-40) with resolution of 0.1 A/m under a field of 800 A/m and an impedance analyzer (Agilent 4294A) with high resolution under a field of 1 A/m at 1 kHz, respectively. A vibrating sample magnetometer (VSM, Lake shore 7410) with resolution of 0.001 T was used to measure the B_s under an applied field of 800 kA/m. Ribbons for

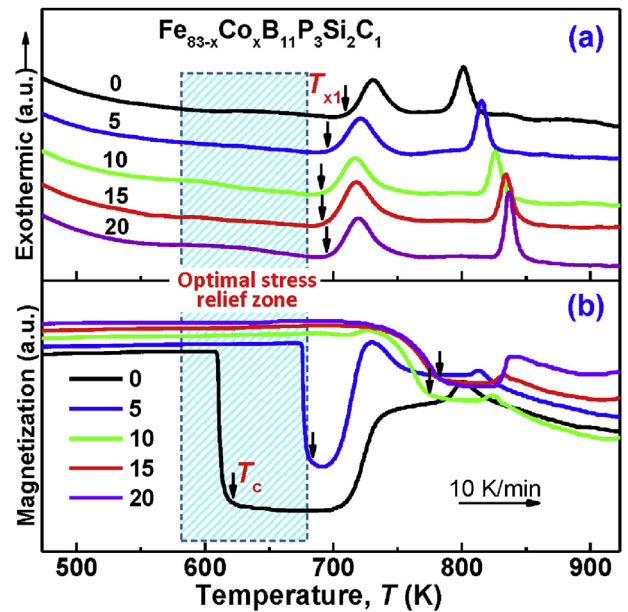


Fig. 1. (a) DTA and (b) TG curves of $\text{Fe}_{83-x}\text{Co}_x\text{B}_{11}\text{P}_3\text{Si}_2\text{C}_1$ as-quenched (AQ) ribbons.

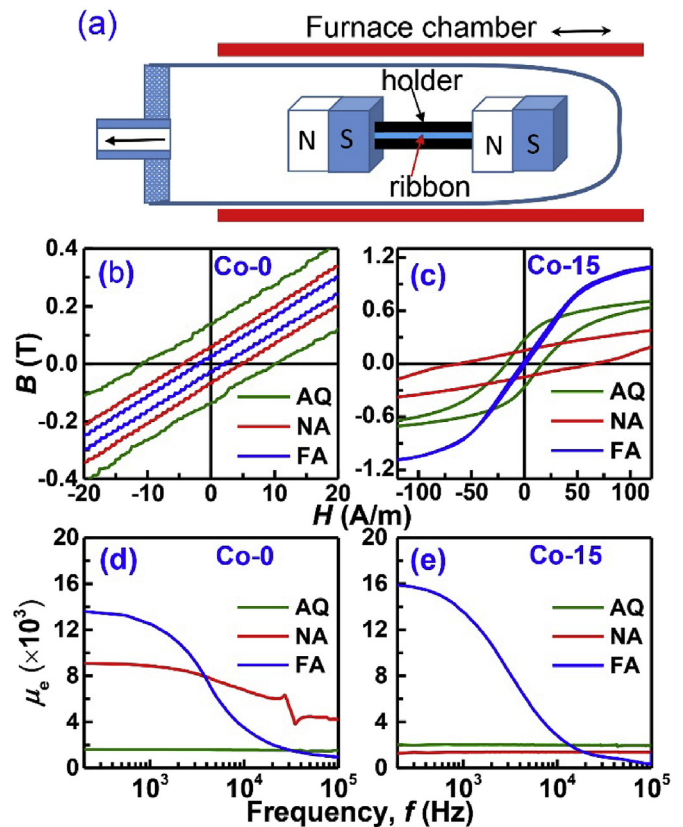


Fig. 2. (a) Schematic diagram of field annealing (FA); (b, c) B-H loop; and (d, e) permeability dependence on frequency of $\text{Fe}_{83}\text{B}_{11}\text{P}_3\text{Si}_2\text{C}_1$ (Co-0) and $\text{Fe}_{68}\text{Co}_{15}\text{B}_{11}\text{P}_3\text{Si}_2\text{C}_1$ (Co-15) amorphous alloy ribbons with as-quenched (AQ), normal annealing (NA) and FA states.

VSM were cut to pieces with length of about 3 mm, fixed on the specimen holder, and were measured after calibrating with a standard Ni sample. All SMPs measurements were applied at room temperature. The microstructures of AQ, NA and FA samples were

identified by X-ray diffraction (XRD, Bruker D8 ADVANCE) with Cu K_{α} radiation, taking 0.2 s for one step of 0.02° . Thermal parameters were examined by differential scanning calorimeter (DSC, Netzsch 404C) at heating rate of 40 K/min with protection of Ar. The microstructures were characterized by transmission electron microscopy (TEM, FEI TF 20) with high resolution transmission electron microscopy (HRTEM) and selected area electron diffraction (SAED).

3. Results and discussions

Thermal parameters of $\text{Fe}_{83-x}\text{Co}_x\text{B}_{11}\text{P}_3\text{Si}_2\text{C}_1$ ($x = 0-20$) amorphous alloy ribbons were conducted by TG/DTA. Fig. 1 (a) showed representative heating curves of amorphous alloys with two crystallization peaks. The onset temperature of the first crystallization (T_{x1}) decreases gradually for alloys with Co content of $x = 0$ to $x = 10$, while increases slightly with further increase of Co to $x = 20$. The Curie transition temperature (T_c) of the amorphous alloys, determined by the sharp loss of magnetization curves in Fig. 1 (b), increases drastically and exceeds the T_{x1} with the increase of Co content to $x = 10$. It should be noticed that the magnetization curves for T_c determination by TG cannot reflect the magnetization decline at the temperature below T_c [17]. According to our previous results of SMPs dependence on the annealing temperature (T_A) [10], the optimal stress relief region was between 570 and 680 K. The alloy without Co addition has changed into paramagnetic or poor ferromagnetic state at the optimal stress relief zone [10,18] and will suffer a normal relaxation process, which result in a sufficient internal stress relief without crystallization. On the contrary, it is concluded that the structure relaxation and crystallization of alloys with $x = 10-20$ are affected by the strong inner magnetic field.

Then, the magnetic properties of the samples conducted to NA and FA were investigated in detail. To manifest the annealing effect, the as-quenched samples were also measured. FA is performed under an applied field of about 200 Oe which is easy to access, as illustrated in Fig. 2 (a). After trying different annealing temperature (T_A) in the optimal stress relief zone, we obtained similar results for the alloys with different Co content. In this context, we show the optimal and representative results of NA and FA samples annealed at 633 K for 15 min. The B-H loops and μ_e vs frequency curves of the representative Co-0 and Co-15 alloys with AQ, NA and FA states were shown in Fig. 2 (b–e). For Co-0 amorphous alloys, both NA and FA can improve the H_c and μ_e as shown in Fig. 2 (b) and (d). For Co-15 samples, NA ribbons showed deteriorated SMPs containing much larger H_c and lower μ_e even than AQ ones, as shown in Fig. 2 (c) and (e). On the contrary, the SMPs of the FA samples were obviously improved, containing extremely low H_c of 1.0 A/m and high μ_e of $16-13.5 \times 10^3$ at 200–1 kHz, which were much better than the NA Co-15 sample and NA/FA Co-0 samples. It is hence verified that the inner and applied magnetic fields have large influence on the SMPs and the FA is an effective method for improving the SMPs, especially for the high Co content alloys with high T_c .

The Co content dependences of H_c , μ_e at 1 kHz and B_s of the amorphous alloys with different $T_{x1} - T_c$ values after NA and FA were systematically shown in Fig. 3. Compared with the AQ samples, NA samples of the alloys with $x = 0$ to $x = 5$ exhibit much lower H_c of 3.3–5.7 A/m and higher μ_e of $6.2-9.1 \times 10^3$, while NA samples of the alloys with $x = 10-20$ exhibit inferior SMPs. For the FA samples, the SMPs are much better than that of the NA and AQ ones. All these results further demonstrate that there are strong correlations between annealing induced structural relaxation determined SMPs and inner/applied magnetic fields. In the whole, the inner magnetic field deteriorates the SMPs and the applied longitudinal one improves the SMPs. The interaction between inner and applied magnetic field enhances the great effect. The B_s reflecting the

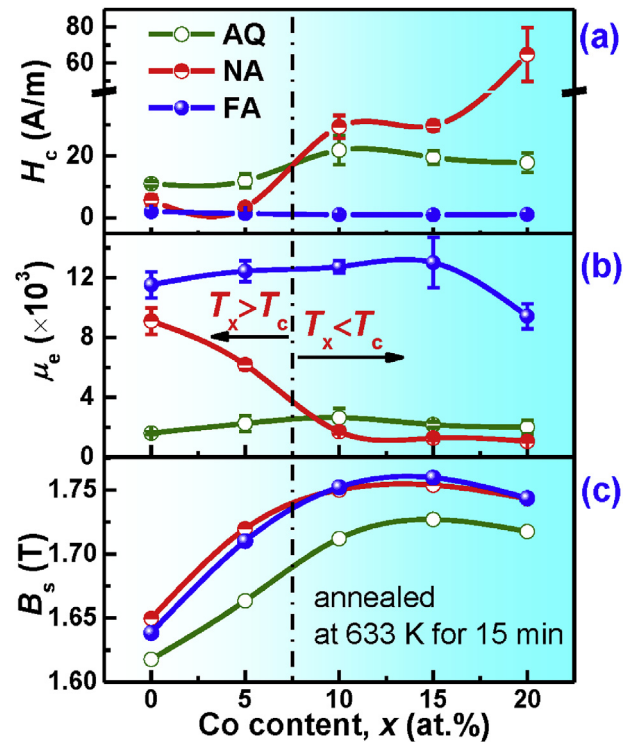


Fig. 3. Co content dependence of H_c , μ_e at 1 kHz and B_s of $\text{Fe}_{83-x}\text{Co}_x\text{B}_{11}\text{P}_3\text{Si}_2\text{C}_1$ ($x = 0-20$) amorphous alloy ribbons with AQ, NA and FA states.

magnetic interaction between Fe atoms and electric structure was firstly investigated. After annealing, the B_s of all alloys increase, illustrating the relaxation induced structural densification [19]. In addition, the B_s of the FA and NA alloy samples show slight changes, indicating that the inner and applied magnetic fields do not change the structural densification nature.

To figure out the reasons of the different SMPs, magnetic domain patterns of Co-0 and Co-15 ribbons with the AQ, NA and FA states were observed and shown in Fig. 4. For the AQ Co-0 and Co-15 samples, domains with transversal sensitive direction are clearly seen on the surfaces. The irregular edge can be illuminated after proper annealing that illustrates the strong pinning effects, which are attributed to the inner stress [20]. As documented, the sensitive direction of the domain reflects the easy magnetization direction [21]. After NA, the domain of Co-0 sample changes into regular strip pattern with large width, indicating the low domain energy and homogenous structure and low stress state. In addition, the sensitive direction of the domains changes to be parallel to the ribbon direction. On the contrary, more domain branching and swerve are seen in the NA Co-15 sample, without sensitive direction change, exhibiting pinning effect. As for FA Co-0 and Co-15 samples, the domains with magnetization along the ribbon axis and smooth edges well explain the excellent SMPs. The domain pattern change is consistent with the SMP results, and further classifies the effects of interaction between inner and applied magnetic field. Here, we must recall that the magnetic domain characterization by using MOKE is a macroscopic technique only reveal the average behavior of the magnetic atoms. It is necessary to further study the magnetization vector arrangement by using a Mössbauer spectra and atomic scale structure by using neutron scattering or synchrotron radiation, for thoroughly reveal the mechanism of this interesting finding. Nevertheless, we can still have a simple understanding according to the documented works. It has been reported that the complex anisotropy distribution is caused by the

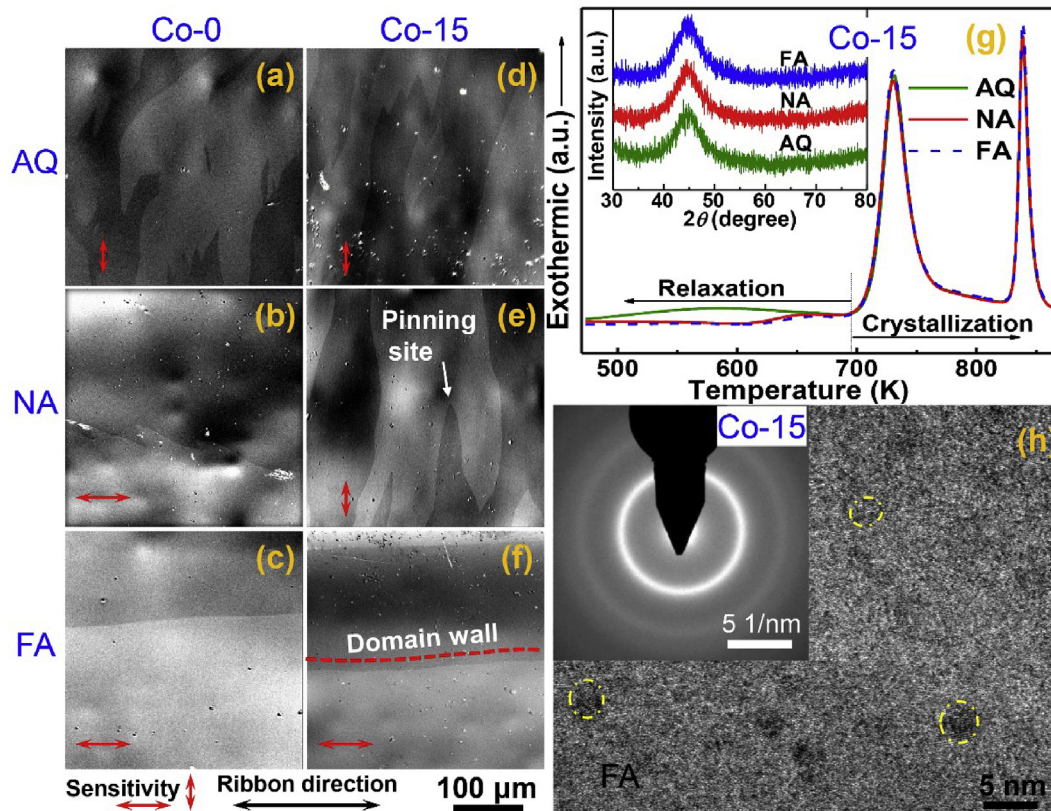


Fig. 4. (a–f) Magnetic domain patterns of Co-0 and Co-15 ribbon samples with AQ, NA and FA states; (g) DSC curves and XRD patterns (inset) of samples with AQ, NA and FA states; (h) HRTEM and SAED of the FA sample.

internal stresses induced during the quenching process [22], in the $\text{Fe}_{78}\text{Si}_9\text{B}_{13}$ alloy ribbon. After NA, individual magnetic moments studied by using a Mössbauer spectrometry are positioned almost perpendicular to the ribbon plane [22]. Pankhurst et al. investigated the moment canting and structural anisotropy of the NA and FA $\text{Fe}_{78}\text{Si}_9\text{B}_{13}$ amorphous alloy ribbons, by using synchrotron Mössbauer radiation. They also found that the structural anisotropy and moment canting are controlled by the strain and directions of the applied magnetic field [23]. We can therefore say that the complex effects of stress and inner/applied have large influence on and can be used to adjust the SMPs of different amorphous alloys.

Since the amorphicity of ribbons will greatly affects the SMPs, the AQ, NA and FA ribbons were identified as amorphous structure in three different ways. DSC measurement in Fig. 4 (g) which was commonly used to identify the relaxation from nanocrystallization was also conducted, for the Co-15 alloy. It is clear that the two crystallization peaks in these three DSC curves show negligible difference, indicating that no obvious nanocrystallization happens for all of the annealed samples. In the low temperature region corresponding to the structural relaxation, the DSC curves of the annealed samples show distinct difference compared with the AQ one, illustrating the adequate relaxation. It is also found that the relaxation region in DSC curves of the NA and FA samples show no difference. The amorphous structure of the samples was also identified according to the XRD patterns shown in inset of Fig. 4 (g). The HRTEM and SAED were also used to investigate the microstructure of a sample after FA. Typical amorphous structure with slight clusters are shown in the HRTEM image in Fig. 4 (h), which is also proved by the inserted SAED image. It is hence concluded that no obvious microstructure change like crystallization happens after FA and NA. The inner and applied magnetic fields during annealing

process will not affect the microstructure.

Now let us discuss the underlying mechanism of our experimental observations about the strong correlations between structural relaxation determined SMPs and inner/applied magnetic fields. As well proposed, the structure of AQ amorphous alloys depicted in Fig. 5 (a) is intrinsically heterogeneous, comprising loose and dense packing regions at the nanoscale in the amorphous matrix [24]. Furthermore, the amorphous state solidified quickly from the melt is far-from-equilibrium and unstable, which is prone to relax towards low energy states [24]. It is well known that annealing below the glass transition temperature can cause relaxation towards the equilibrium state and a more homogeneous structure [25]. The relaxation process, which is currently a research hotspot and complicated issue [26], is argued to comprise α and β modes correlated to the multiple behaviors such as amorphous alloy relaxation shear transformation zone activation, small atom diffusion, macroscopic tensile plasticity and structural heterogeneity, etc. [27,28]. To simplify and find a feasible method towards this critical issue, here, we discard the complicated and controversial relaxation modes, and just consider the homogenization effects of structure, stress relief and magnetic anisotropy changes, which are reported to dominantly determine the SMPs [20,29,30]. Beside the structure heterogeneity existed in all amorphous alloys, the ferromagnetic samples also possess stress and magnetic heterogeneity, which interact and have great influence on the relaxation process. Compared with the nano-scaled loose/dense packing regions, the magnetic domain with different magnetic field directions are much larger, as shown in Fig. 5. According to our former results, the magnetic field is the key factor determining the SMPs and hence focused in this study.

For the alloys with $T_c < T_{X1}$, the amorphous samples under

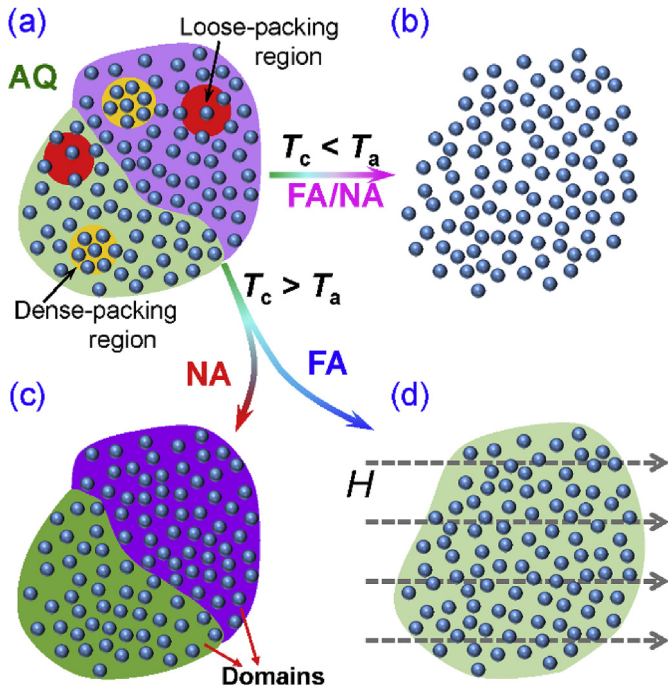


Fig. 5. Schematic diagram of microstructure changes in the AQ, NA and FA samples.

annealing transit to paramagnetic state and are no longer affected by the inner magnetic field at optimal stress relief temperature. In the annealing induced relaxation process shown in Fig. 5 (b), the microstructure is homogenized and densified, which results in the decrease of pinning sites and increase of the exchange coupling between Fe atoms [16]. In addition, the strong inner stress derived from the fast and non-uniform cooling process is eliminated, which will greatly decrease the magnetic anisotropy. All these will give sufficient explanation for the improvement in SMPs and B_s of the NA samples. For the FA, one can envisage that one hand alone can't clap, at optimal stress relief temperature. The slight improvement of SMPs of the alloys with $T_c < T_{x1}$ by FA can be attributed to the domain formation during the cooling process.

For the NA samples with $T_c > T_{x1}$, the relaxation process is affected by the inner magnetic field, as shown in Fig. 5 (c). Though the local microstructure is also relaxed by the thermal excitation, the macroscopic structure in different magnetic environment will differ more considerably. Owing to the irregular domain patterns of the AQ samples, the inner magnetic field are complicated. The annealing induced relaxation will aggregate the influence of inner magnetic field and lead to a higher magnetic anisotropy, which is the reason why the NA samples exhibit worse SMPs than the AQ ones.

For the FA samples with $T_c > T_{x1}$, the magnetic domain is originated before and during the annealing process by the applied longitudinal magnetic field. The structure will relax to be locally homogeneous and macroscopically originated to applied magnetic field direction. The easy magnetization direction as identified by Fig. 4 will be modulated to be parallel to the ribbon direction, which is propitious to improve the SMPs. The interaction between the inner and applied fields is used for the magnetic domain origination and microstructure adjustment during annealing induced relaxation.

The anisotropy should also be considered when explaining the different SMPs behavior among the AQ, NA and FA samples. It is well accepted that the AQ sample combines a stress-induced anisotropy. After NA process, the stress-induced anisotropy of the

samples with low T_c should decrease for the inner stress alleviation. For the amorphous alloys with high $T_c (> T_{x1})$, NA samples acquired stabilization of magnetic domain and anisotropy. According to the domain patterns in Fig. 4, the anisotropy was still in the transversal direction. On the contrary, the FA could result in a uniaxial anisotropy along the ribbon axis [31]. This direction was in consistent with the applied field direction during test, which results in the great improvement of the SMPs after FA.

At last, we summarize the effects of NA and FA on SMPs. The annealing leads to structure relaxation which results in a locally homogenous microstructure. The excellent SMPs of the NA and FA samples with $T_c < T_{x1}$ is attributed to the low magnetic anisotropy and pinning effects. The samples with $T_c > T_{x1}$ will be macroscopically non-uniform under the action of inner magnetic field, during the NA. The structure will relax to be locally homogeneous and macroscopically originated to applied magnetic field direction, for the $T_c > T_{x1}$ samples subjected to FA. It should be noted that these conclusions are withdrawn from the results of Co added alloys with different $T_{x1} - T_c$, but will not restricted to these alloys. The situations like annealing low T_c samples at lower temperature are also a coincidence. Nevertheless, there is still no detailed physical picture of the relaxation process of ferromagnetic amorphous alloys and therefore it is still an open question.

4. Conclusions

Longitudinal field annealing (FA) is used to improve the SMPs of $\text{Fe}_{83-x}\text{Co}_x\text{B}_{11}\text{P}_3\text{Si}_2\text{C}_1$ ($x = 0-20$) high B_s amorphous alloy ribbons with thickness of 25 μm produced with melt spinning technique. The underlying mechanism of the strong correlations between structural-relaxation determined SMPs and inner/applied magnetic fields is discussed. The main conclusions are as follows:

- 1) FA is effective in improving SMPs (H_c and μ_e) both for low and high T_c amorphous alloys. The $\text{Fe}_{83-x}\text{Co}_x\text{B}_{11}\text{P}_3\text{Si}_2\text{C}_1$ ($x = 0-20$) amorphous alloys achieve combining of high B_s of 1.65–1.76 T, low H_c of 1.0–2.3 A/m and high μ_e of $6.6-13 \times 10^3$ at 1 kHz.
- 2) For the samples with $T_c < T_{x1}$, the excellent SMPs of the NA and FA are attributed to the low magnetic anisotropy and pinning effects. For the samples with $T_c > T_{x1}$, NA gets macroscopically non-uniform under the action of inner magnetic field; while FA manipulates domain structure from transversal to along with ribbon axis, and simultaneously relaxes to be locally homogeneous and macroscopically originated to applied magnetic field direction.

Acknowledgement

This work was supported by the National Key Research and Development Program of China (2016YFB0300501, 2017YFB0903902), the National Natural Science Foundation of China (Grant No. 51601206, 51771159). This work was also supported by General Research Fund of Hong Kong under the grant number of CityU 102013.

References

- [1] R. Hasegawa, *Mater. Sci. Eng., A* 375–377 (2004) 90–97.
- [2] D.H. Milanez, L.L. Faria, D.R. Leiva, C.S. Kiminami, W.J. Botta, *J. Alloy. Comp.* 716 (2017) 330–335.
- [3] R. Hasegawa, D. Azuma, *J. Magn. Magn. Mater.* 320 (2008) 2451–2456.
- [4] Y. Ogawa, M. Naoe, Y. Yoshizawa, R. Hasegawa, *J. Magn. Magn. Mater.* 304 (2006) e675–e677.
- [5] T. Hibino, T. Bitoh, *J. Alloy. Comp.* 707 (2017) 82–86.
- [6] J.H. Zhang, C.T. Chang, A.D. Wang, B.L. Shen, *J. Non-Cryst. Solids* 358 (2012) 1443–1446.
- [7] K. Xu, H.B. Ling, Q. Li, J.F. Li, K.F. Yao, S.F. Guo, *Intermetallics* 51 (2014) 53–58.

- [8] K. Suzuki, A. Makino, A. Inoue, T. Masumoto, *J. Appl. Phys.* 70 (1991) 6232–6237.
- [9] J.-F. Li, Y. Shao, X. Liu, K.-F. Yao, *Sci. Bull.* 60 (2015) 396–399.
- [10] C.L. Zhao, A.D. Wang, A.N. He, S.Q. Yue, C.T. Chang, X.M. Wang, R.-W. Li, *J. Alloy. Comp.* 659 (2016) 193–197.
- [11] B.L. Shen, A. Inoue, C.T. Chang, *Appl. Phys. Lett.* 85 (2004) 4911–4913.
- [12] F. Jia, W. Zhang, X.G. Zhang, G.Q. Xie, H. Kimura, A. Makino, A. Inoue, *J. Alloy. Comp.* 504 (2010) S129–S131.
- [13] Y. Han, J. Ding, F.L. Kong, A. Inoue, S.L. Zhu, Z. Wang, E. Shalaan, F. Al-Marzouki, *J. Alloy. Comp.* 691 (2017) 364–368.
- [14] H. Chiriac, N. Lupu, *J. Magn. Magn. Mater.* 215 (2000) 394–396.
- [15] V.V. Shulika, A.P. Potapov, *J. Phys.* IV 08 (1998) 147–150.
- [16] H. Kronmüller, B. Gröger, *J. Phys.* 42 (1981) 1285–1292.
- [17] Q. Zheng, L. Zhang, J. Du, *Scripta Mater.* 130 (2017) 170–173.
- [18] C. Kittel, *Introduction to Solid State Physics*, Wiley, New York, 1996.
- [19] M. Dokukin, N. Perov, A. Beskrovnyi, E. Dokukin, *J. Magn. Magn. Mater.* 272 (2004) e1151–e1152.
- [20] H. Kronmüller, *J. Appl. Phys.* 52 (1981) 1859–1864.
- [21] J.D. Livingston, *Phys. Status Solidi* 70 (1982) 591–596.
- [22] N. Amini, M. Miglierini, M. Hasiak, J. Dekan, S. Habibi, *Acta Phys. Pol. A* 131 (2017) 666–668.
- [23] Q.A. Pankhurst, N.S. Cohen, L.F. Barquin, M.R.J. Gibbs, G.V. Smirnov, *J. Non-Cryst. Solids* 287 (2001) 81–87.
- [24] Y. Yang, J.F. Zeng, A. Volland, J.J. Blandin, S. Gravier, C.T. Liu, *Acta Mater.* 60 (2012) 5260–5272.
- [25] J.Q. Wang, Y. Shen, J.H. Perepezko, M.D. Ediger, *Acta Mater.* 104 (2016) 25–32.
- [26] Q. Wang, J.J. Liu, Y.F. Ye, T.T. Liu, S. Wang, C.T. Liu, J. Lu, Y. Yang, *Mater. Today* 20 (2017) 293–300.
- [27] W.H. Wang, Y. Yang, T.G. Nieh, C.T. Liu, *Intermetallics* 67 (2015) 81–86.
- [28] H.-B. Yu, W.-H. Wang, K. Samwer, *Mater. Today* 16 (2013) 183–191.
- [29] P. Allia, F. Vinai, *IEEE Trans. Magn.* 14 (1978) 1050–1053.
- [30] N. Bayri, V.S. Kolat, F.E. Atalay, S. Atalay, *J. Phys. D Appl. Phys.* 37 (2004) 3067–3072.
- [31] R. Sommer, C. Chien, *Appl. Phys. Lett.* 67 (1995) 857–859.